Figure 6.3 Profiles of zonal wind stress from 100 to 120°W, illustrating the annual cycle. To emphasize the meridional structure, the weak monthly mean value of the equatorial stress (the average of figures 6.1i and 6.1j) was subtracted from the monthly mean value at each latitude.

6.3 Theories

6.3.1 Integrated Theories

The earliest theoretical attempts sought an explanation for the North Equatorial Countercurrent. This current defies intuition since it flows opposite to the prevailing winds. Montgomery and Palmén (1940) suggested that the easterly wind stress in the equatorial zone is balanced by the vertically integrated zonal pressure gradient. They presented supporting observational evidence in the Atlantic. One interesting result was their demonstration that the baroclinic pressure gradients generally were confined to the top few hundred meters of the water column. As an explanation for the North Equatorial Countercurrent, they hypothesized that in the doldrums, i.e., in the vicinity of the ITCZ, where the magnitude of the zonal stress is greatly reduced, the pressure gradient would maintain the value that it had on either side of this region and hence no longer be balanced by the wind stress. As a result, an eastward flow would develop, which they suggested would be retarded by lateral friction. Charts of dynamic topography (Tsuchiya, 1968) indicate that the zonal pressure gradient in this region is, in fact, less than it is farther to the north and south. Furthermore, since 1° or 2° off the equator Coriolis terms cannot be neglected and

the depth-integrated value of the meridional velocity usually does not vanish, the suggestion of Montgomery and Palmen (1940) does not represent a proper explanation for the North Equatorial Countercurrent.

Sverdrup (1947) suggested that the North Equatorial Countercurrent was not only a consequence of the zonal wind stress but also was related to the curl of the wind stress and continuity requirements. He assumed in his model that the currents were steady and vanished at a deep level. The equations were integrated from this depth to the sea surface; hence the solution gave no information about the vertical structure of the motion field. The apparent success of Sverdrup's theory in the eastern Pacific is often cited as observational endorsement of its widespread use in large-scale ocean-circulation theory.

In light of the earlier discussion about the large variability in the position and amplitude of the NECC, and the considerable monthly variation in the winds in this region, it is surprising that this steady theory should be applicable there. In fact, Sverdrup (1947) and Reid (1948), instead of using the mean wind stress in their computations, used the October–November values. They also used October–November oceanographic data to compute vertically integrated pressure. Implicit in their theory, then, was the assumption that the oceanic response to the fluctuating winds was sufficiently rapid that the ocean was almost always in equilibrium with the instantaneous winds (i.e., quasi-steady).

Therefore, it is of some interest to redo the computations of Sverdrup and Reid using the values for the monthly mean stress field from Wyrtki and Meyers (1975) and to compare the results with oceanographic data from different times of the year to see whether Sverdrup balance really is quasi-steady. The monthly values of the zonal Sverdrup transport are shown in figure 6.4. The October and November curves look quite similar to those of Sverdrup. The overall spatial and temporal evolution of the currents throughout the year resembles the picture that has been derived for the surface flow field from ship-drift observations. It is possible to check to see whether the historical integrated geostrophic transports follow a similar pattern of change.

During 1967 and the first part of 1968, hydrographic sections at four different longitudes between 100 and 120°W were occupied across the equator at seven different times. The geostrophic velocity computations relative to 500 db for these sections are given by Love (1972). Using these figures, the geostrophic transport for 2° bands of latitude from 2 to 12°N was computed by a planimetric integration. The minimum contour interval for the velocities was $5\ \mathrm{cm\,s^{-1}}$; this interval introduces an uncertainty of about $3 \times 10^9\ \mathrm{kg\,s^{-1}}$ into
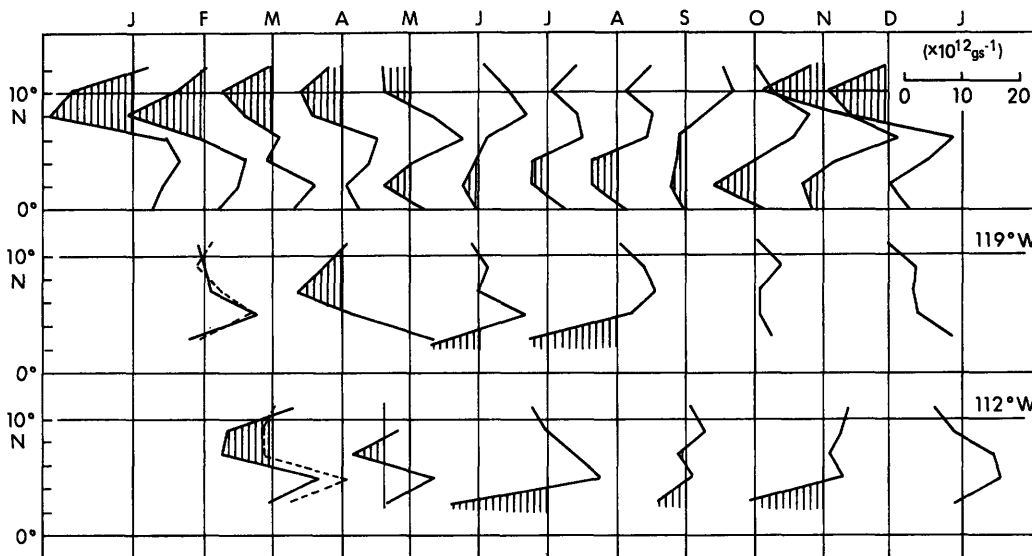
A. Leetmaa, J. P. McCreary, Jr., and D. W. Moore

Figure 6.4 Upper panel depicts monthly Sverdrup transport. Lower two panels show geostrophic transports observed during the EASTROPAC expedition.

each transport computation (2.5 cm s^{-1} × 500 m × 2° × 1 g cm^{-3}). The results of these integrations for the sections at 119°W and 112°W are shown in figure 6.4. The tendency at both sections is for the transport in the south equatorial current to be strongest during the summer. The NECC lies close to the equator early in the year and moves northward during the summer and southward again during late fall. The transport patterns at both sections during the first part of 1967 and 1968 are quite similar. This agreement could be coincidence or indicate that these fluctuations perhaps have a regular annual cycle. The observed geostrophic transport patterns are visually similar to the theoretical pattern; there clearly are quantitative differences, however.

The important conclusion from this study is that it cannot be said whether the Sverdrup relation provides an accurate description of the currents in the eastern tropical Pacific. Sverdrup and Reid were probably fortunate in that their results seemed to agree so well with observations. The real problem with testing Sverdrup theory, in light of what we now know about barotropic and baroclinic adjustment, is associated with the assumed level of no motion. For an ocean with a free-slip flat bottom, Sverdrup balance should hold for the integrated flows and pressures, as long as the integral goes all the way to the bottom and barotropic adjustment has had time to occur (approximately a few days). If the integration extends only over the surface layers (upper 500 or 1000 m, say), however, then integrated quantities depend on both the barotropic and baroclinic components, and a quasi-steady theory will apply only if the dominant baroclinic modes have also reached equilibrium. In general for the annual cycle, there is no reason this should be true since baro-clinic adjustment even near the equator takes at least a few months. Clearly what is needed is an understanding of baroclinic adjustment processes.

6.3.2 Baroclinic Theories

The discovery of the Equatorial Undercurrent in the Pacific in 1952 (Cromwell, Montgomery, and Stroup, 1954) triggered a great deal of equatorial modeling activity in the latter part of that decade. Almost all of these early models include baroclinic effects in a crude way by assuming the surface layer is essentially decoupled from the deep ocean below (Yoshida, 1959; Stommel, 1960; Charney, 1960). Another assumption common to these models is that all fields except the pressure are assumed to be independent of x, the east-west coordinate; the zonal pressure gradient $\partial p / \partial x$ is taken to be a constant related to the zonal wind stress that is driving the motion.

The simplest and most elegant of these models is that of Stommel (1960). This model is the first successful extension of classical Ekman theory to the equator. Stommel's model equations balance the Coriolis force with vertical diffusion of momentum (the Ekman balance) while retaining horizontal pressure gradients. It is the zonal pressure gradient which allows him to avoid the equatorial singularity of previous Ekman theory, and which provides a source of eastward momentum to drive the undercurrent. The wind forcing is put into the ocean as a surface stress, and a zero-stress condition is imposed at the bottom of the layer. The vertical structure of the zonal velocity at the equator is parabolic, with surface flow in the direction of the wind and subsurface flow (undercurrent) in the opposite direction. In addition, the model develops a meridional circulation very similar to that hypothe-

189
Equatorial Currents

sized by Cromwell to account for the distribution of tracers in the equatorial Pacific (Cromwell, 1953). Figure 6.5, by Stommel (1960), illustrates the circulation pattern developed by his model. There is surface divergence of fluid from the equator, subsurface convergence, and equatorial upwelling. A major drawback of this theory is that the response is too closely related to the choice of eddy viscosity ν. Let U and L represent the velocity and depth scales of the flow and τ measure the equatorial zonal wind stress. Let H be the depth of the layer and β be the meridional derivative of the Coriolis parameter. Then in the Stommel model

$$U = \frac{H\tau}{\nu} \quad \text{and} \quad L = \frac{\nu}{\beta H^2} . \quad (6.1)$$

It is not possible to select a value for ν which simultaneously sets a realistic magnitude as well as width scale for the flow. In particular, if ν is adjusted so that the current has a reasonable speed, then it is far too narrow.

Charney's (1960) nonlinear model differs fundamentally from Stommel's in that he requires a no-slip bottom boundary condition. Because of this stringent condition, the linear model cannot produce any flow counter to wind, and so it is clearly the presence of nonlinearities that allows the model to generate an undercurrent. Charney computed the zonal and vertical velocity only on the equator. Later, Charney and Spiegel (1971) extended the model off the equator to determine the flow field in a meridional section and also obtained the same general pattern of meridional circulation as that proposed by Cromwell. They explained the existence of an undercurrent in both models in the following qualitative manner [first suggested by Fofonoff and Montgomery (1955)]. Fluid converging toward the equator conserves absolute vorticity. As a result, planetary vorticity is converted to relative vorticity, and this conversion provides an additional source of eastward momentum to drive the
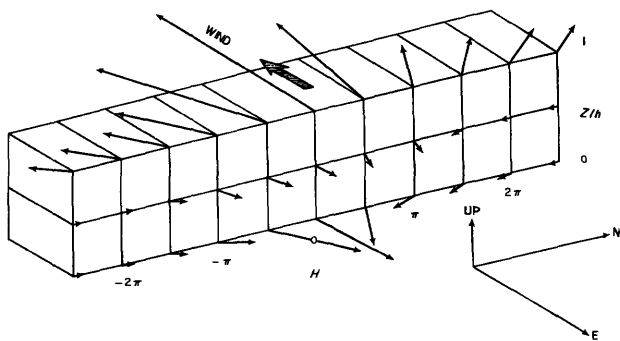

Figure 6.5 Schematic three-dimensional diagram of the flow field in the neighborhood of the equator, not showing the vertical component of velocity, which can in principle be determined from continuity. (After Stommel, 1960.)

undercurrent. These studies show that nonlinearities are likely to play an important role in equatorial dynamics. On the other hand, the nonlinear solutions are even more sensitive to the choice of ν than Stommel's linear one. For example, when ν decreases from 17 to 14 cm^{2}s^{-1}, the speed of the Equatorial Undercurrent more than doubles, and the e-folding width of the jet narrows significantly.

Other workers subsequently considered similar layer models and explored the importance of terms in the equations of motion that were ignored in the earlier studies (Philander, 1973; Cane, 1979b). Despite their successes, the layer models have obvious limitations. The assumption of an x-independent flow field is questionable, the decoupling of the lower layer is highly artificial, and the solutions are extremely dependent on the choice of mixing coefficients. Finally, the observations themselves suggest the most serious drawback. Although an undercurrent has been observed in the mixed layer (see for example Hisard, Merle, and Voituriez, 1970), the strongest eastward flow is almost always found in the thermocline below the surface mixed layer. Therefore, an undercurrent model that treats the effects of stratification in a more realistic way is required. It took another decade for such a model to be developed, and the development proceeded from an entirely different direction, namely, from attempts to understand time-dependent processes in the equatorial region.

Initial interest in equatorial waves was largely theoretical, and grew out of attempts to extend the theory of midlatitude gravity and Rossby waves to the equator. Longuet-Higgins (1964, 1965, 1968a) undertook a detailed investigation of planetary waves on a rotating sphere (cf. chapters 10 and 11). At about the same time, Blandford (1966) and Matsuno (1966) both used equatorial β-plane models (i.e., the Coriolis parameter is approximated by $f = \beta y$) to describe free baroclinic waves. [Groves (1955) had earlier derived the same β-plane equatorially trapped solutions as Blandford and Matsuno, but he was considering barotropic tides.] All of these studies are linear and inviscid, and consider perturbations on a background state consisting of a stably stratified ocean at rest. Normal modes for the vertical structure of the fields are derived just as Fjeldstad (1933) originally did for internal waves. The eigenvalues for the vertical separation problem are usually presented as equivalent depths h' for the resulting normal modes. In general, for a finite depth ocean, there is one barotropic mode for which the equivalent depth is nearly equal to the actual depth of the ocean, and the corresponding eigenfunction describing the depth dependence of the horizontal velocities and pressure perturbation is nearly depth independent. There is also a denumerably infinite set of baroclinic equivalent

A. Leetmaa, J. P. McCreary, Jr., and D. W. Moore

depths. The vertical structures of the baroclinic eigenfunctions depend on the details of the background density distribution. For each equivalent depth h', there is a corresponding phase speed c defined by $c^2 = gh'$.

With this separation, the horizontal and time dependence of each vertical mode of the system can now be investigated independently of the z-dependence. If c is the phase speed for the mode in question, then free oscillations at frequency ω can exist in a latitudinal band, $|y| \leq y_T$. In the equatorial β-plane model, the turning latitude is given by

$$y_T = \left(\frac{\omega^2}{\beta^2} + \frac{c^2}{4\omega^2} \right)^{1/2} \tag{6.2}$$

and is strongly dependent on ω. For the first baroclinic mode, c is typically about 250 cm s^{-1}. Then at the annual cycle, $y_T = 6250$ km; at the 5-day period $y_T = 640$ km, a much smaller trapping scale. [For a complete discussion of free equatorial trapped waves see Moore and Philander (1977) and chapter 10.]

Moore (1968) investigated the effects of oceanic boundaries on free waves at frequencies corresponding to strong equatorial trapping (near-minimum y_T for a given value of c). He showed that a Kelvin wave at frequency ω hitting an eastern boundary will generally reflect some of its energy back in the form of equatorially trapped Rossby waves, and the rest of the energy propagates poleward as coastally trapped Kelvin waves. These results were later extended to the case of an incoming Kelvin wave of step-function form by Anderson and Rowlands (1976a).

The first observational evidence—in Pacific sea-level variations—for the existence of strongly equatorially trapped baroclinic waves in the ocean was presented by Wunsch and Gill (1976). Spectral peaks corresponding to periods in the range 2-7 days were explained in terms of equatorially trapped inertial-gravity waves with vanishing east-west group velocity. The variation in the strength of the spectral peaks from islands at different latitudes was consistent with the expected latitudinal structure of the theoretical wave modes (see figure 10.11). Additional observational evidence for equatorially trapped waves was provided by Harvey and Patzert (1976) from deep mooring data in the eastern equatorial Pacific. Weisberg, Miller, Horigan, and Knauss (1980) and Weisberg, Horigan, and Colin (1979) did the same using Atlantic GATE data and later Gulf of Guinea observations.

An interesting property of the low-frequency large-scale baroclinic waves (nearly nondispersive Rossby waves) is that their phase speed increases markedly the more trapped they are to the equator. The swiftest wave, the equatorial Kelvin wave, is also the most strongly trapped. This property suggests that the forced baroclinic response of the equatorial ocean need not remain locally confined to the forcing region, but can radiate swiftly away. That is to say, baroclinic effects may be remotely as well as locally forced.

In 1969, Lighthill published a seminal paper entitled "Dynamic Response of the Indian Ocean to the Onset of the Southwest Monsoon." He was motivated by the idea that the Somali Current might be remotely forced by winds in the interior of the Indian Ocean. He coupled the wind stress to the model ocean in a novel way, not as a surface condition, but rather as a body force uniformly distributed throughout an upper mixed layer. This approach avoids the details of the frictional processes by which the stress actually enters the ocean and allows the use of the inviscid normal modes to study the oceanic response to variable wind forcing. The model ocean is forced by an impulsive wind-stress distribution concentrated away from the coast in the center of the Indian Ocean. In addition to the locally forced response, long-wavelength nondispersive Rossby waves are generated at the edge of the forcing region and propagate westward to the coast. They are reflected there as short-wavelength dispersive Rossby waves that remain trapped to the coast. He interpreted the coastal response as the onset of the Somali Current.

One of the most prominent features of the equatorial oceans is the presence of a strong near-surface pycnocline. Observations show that changes in the pycnocline depth can be large and occur very rapidly. It is sensible to model this motion as simply as possible, with either a one-and-a-half-layer model (a single upper moving layer overlying a slightly denser inert layer) or with a two-layer model; in both cases the layer interface plays the role of the pycnocline. Wind stress enters the ocean as a body force in the surface layer, and so such models are analogous to the Lighthill model if it is limited to a single baroclinic mode. Not surprisingly, a large number of these models, both linear and nonlinear, have been used in the past decade to investigate a variety of equatorial adjustment problems.

O'Brien and Hurlburt (1974) used a two-layer model to study the interior response of the equatorial Indian Ocean to change in zonal wind stress. The model produces an eastward equatorial jet with many of the observed features documented by Wyrtki (1973a). The meridional structure of the accelerating jet produced in the O'Brien and Hurlburt model is basically the same as the structure of the surface flow given in Yoshida's (1959) undercurrent paper and has been called the Yoshida jet. See Moore and Philander (1977) for a detailed description of the spin-up of the Yoshida jet from rest for a single inviscid baroclinic mode.

The idea that the Somali Current might be remotely forced stimulated a number of additional studies. Anderson and Rowlands (1976b) used a one-and-a-half-

layer analytical model to investigate the relative importance of local and remote forcing. They concluded that local forcing is initially dominant but that remotely forced effects will ultimately become important. Hurlburt and Thompson (1976) used a two-layer model forced by a basin-wide northward stress τ^y to show that nonlinear advective effects rapidly become important in the developing boundary flow. Cox (1976) addressed the same problem using a more sophisticated 12-level numerical model. His findings corroborate the conclusions of the simpler models.

Hickey (1975) and Wyrtki (1975b) suggested that El Niño occurs in conjunction with a relaxation of the southeast trades in the central and western Equatorial Pacific. Hurlburt, Kindle, and O'Brien (1976) applied substantially the same model as O'Brien and Hurlburt (1974) to simulate the onset of El Niño. They spun-up the model with a uniform westward wind for 50 days, and then turned off the wind. Major features of the response included an eastward-traveling Kelvin wave originating at the western boundary, westward-traveling nondispersive Rossby waves originating at the eastern boundary, and poleward-traveling Kelvin waves along the eastern boundary. The thickening of the warm layer near the eastern boundary in response to the relaxation of the winds demonstrated the plausibility of Wyrtki's hypothesis. Although the model of Hurlburt, Kindle, and O'Brien was nonlinear, the response was completely dominated by linear dynamics. The only discernible nonlinear effect was the steepening front of the poleward-propagating coastal Kelvin wave.

McCreary (1976) used a one-and-a-half-layer linear model in a similar study of El Niño. He followed the initial response of the eastern ocean to various zonally uniform distributions of wind stress. Important conclusions are the following. Changes in the meridional wind field cannot cause an El Niño event. Changes in the zonal wind field outside the equatorial band (roughly ±5° of latitude) are not important in generating El Niño. Finally, model results suggest that the meridional profile of the wind field can significantly affect the resulting flow field. For example, the southward motion of the ITCZ can force southward cross-equatorial transport of water in the eastern Pacific. It is interesting that in this model the deepening of the pycnocline in the eastern Pacific is initiated by the weakening of the local zonal winds, and is stopped by the arrival of an equatorially trapped Kelvin wave from the western ocean.

McCreary (1977, 1978), realizing that the changes in the Pacific wind field during El Niño are not zonally uniform, but rather are confined in the central and western ocean, extended the model of the 1976 study so that a wind-stress patch of limited longitudinal ex-

tent could be imposed. Figure 6.6 shows the adjustment of the model thermocline topography after a weakening of the westward trade winds by an amount +0.5 dyn cm^{-2}. The dotted lines in the upper left panel of the figure delineate the region of weakened trade winds; the wind-stress change is a maximum in the central portion and weakens markedly in the surrounding areas. After 35 days, a downwelling signal rapidly radiates from the region of the wind patch as a packet of equatorially trapped Kelvin waves and already the equatorial thermocline (and also sea level) begins to tilt to generate a zonal pressure gradient that balances the wind there. In the region of strongest wind curl, the thermocline begins to move closer to the surface, and this upwelling signal propagates westward as a packet of Rossby waves. After 69 days, the packet of Kelvin waves has already reflected from, and spread along, the eastern boundary. As time passes, this downwelling signal propagates back into the ocean interior as a packet of Rossby waves, and more and more upper-layer water piles up in the eastern ocean. As shown in the lower two panels, the source of the water is a broad area of the western and central ocean where the thermocline is uplifted; in some regions the thermocline rises over 65 m. Note that in this case it is the arrival of the Kelvin wave that causes the initial deepening of the pycnocline in the eastern ocean. The figure also further demonstrates the importance of knowing the horizontal structure of the wind field; the rapid tilting of the equatorial thermocline, and the form of the extraequatorial upwelling are a direct result of the particular structure chosen here.

Moore et al. (1978) suggested that the equatorial upwelling in the eastern Atlantic and coastal upwelling in the Gulf of Guinea might be a remote response to an increase in the strength of the westward wind stress in the western Atlantic. The variation of $\partial p/\partial x$ in the western Atlantic reported by Katz et al. (1977) was interpreted as the response to such an increase. O'Brien, Adamec, and Moore (1978) and Adamec and O'Brien (1978) used the same basic adjustment model as had been applied earlier to the Indian and Pacific Oceans to study Atlantic adjustment. The ocean geometry is rectangular with a rectangular notch cut out of the northeast corner of the basin to simulate West Africa. The model calculations showed that an increase in strength of the westward wind stress in the western Atlantic generates an equatorial-upwelling response that propagates eastward, leaving behind a thermocline tilt to balance the stress. When it hits the coast, the upwelling signal propagates away from the equator along the boundary and travels westward along the coast of the Gulf of Guinea.

The important role that equatorially trapped waves play in all these models has stimulated several studies

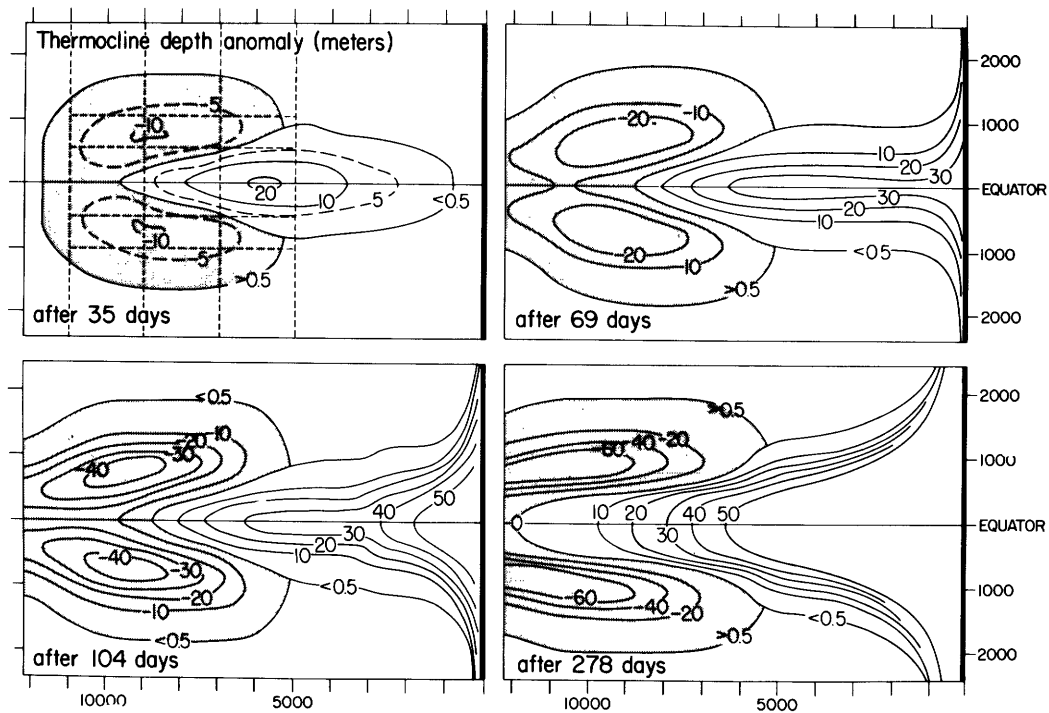A. Leetmaa, J. P. McCreary, Jr., and D. W. Moore

Figure 6.6 Time development of the thermocline depth anomaly to a longitudinally confined zonal wind stress. The dotted lines in the upper left panel indicate the region of the wind. The solid lines in each panel indicate the presence of an eastern ocean boundary. Horizontal distances are in kilometers. (After McCreary, 1977.)

of the interaction of the waves with the mean zonal currents. Hallock (1977) used a two-and-a-half-layer model forced by meridional surface winds to investigate the Equatorial Undercurrent meanders observed during GATE. A meridional stress τ^y with a zonal wavelength of 2400 km is turned on gradually in a few days and then held steady. Part of the response is an equatorially trapped Yanai wave of about 16-day period. The characteristics of this Yanai wave were somewhat, but not drastically, modified by including mean surface currents in the upper layer and a mean undercurrent in the second layer. Thus it was suggested that the GATE observations of Equatorial Undercurrent meanders might be explained in terms of passive advection of the Equatorial Undercurrent by a wind-generated Yanai wave. McPhaden and Knox (1979) and Philander (1979) used one-and-a-half-layer models to study the modifications of other free waves in the presence of various meridional profiles of zonal mean currents. McPhaden and Knox concentrate on the equatorial Kelvin and inertial-gravity waves (including the Yanai wave), and conclude that the zonal velocity associated with a given mode can be strongly modified by the background currents. Philander also considers equatorial Rossby waves and suggests that these waves may be influenced strongly by the presence of the Equatorial Undercurrent.

Philander (1976) used a two-and-a-half-layer model to show that background zonal currents also allow unstable waves and predicted a possible instability of the surface currents in the tropical Pacific. The most unstable waves which propagate westward have a wavelength of about 1000 km and a period of approximately 25 days. The satellite observations of Legeckis (1977b) seem consistent with the instability scales Philander predicted. A later numerical study by Cox (1980) confirmed a suggestion of Philander's that oscillations generated by such surface-current instabilities could propagate zonally for large distances while propagating vertically into the deep ocean. The results indicate that the Harvey and Patzert (1976) observations in the eastern Pacific near the sea floor could, in fact, be such remote effects of surface-current instabilities generated farther to the west.

It is now apparent that simple layer models have been remarkably successful in reproducing many of the obvious features of time-dependent equatorial ocean circulation. These models are intrinsically limited, however, in their ability to describe the vertical structure of the ocean, and recently theoreticians have begun to study more sophisticated models that allow for high vertical resolution. There are several reasons for this interest. In 1975, Luyten and Swallow (1976) discovered high-vertical-wavenumber equatorially trapped multiple jets in the Indian Ocean, and in 1978 similar structures were observed in the Pacific (C. Erik-

sen, personal communication). In addition to this observational impetus, general theoretical questions arise in trying to understand in greater detail just how the wind stress enters the ocean. For example, how valid is the assumption that the wind enters as a body force distributed over a surface mixed layer? Finally, there is the perennial interest in understanding the dynamics of the Equatorial Undercurrent.

In order to model the multiple jets, Wunsch (1977) considered an inviscid continuously stratified model, which he took to be horizontally unbounded and infinitely deep. (At the end of his study he also reported effects introduced by a western ocean boundary.) Since the model was inviscid, it was not possible to introduce the wind stress as a surface boundary condition. Instead, Wunsch assumed that a thin wind-driven surface boundary layer pumped the deeper ocean with a surface distribution of vertical velocity. For convenience, he chose for the form of the distribution a westward-propagating sinusoidal wave. To specify the solution, he required it to match this vertical velocity distribution at the ocean surface and also to exhibit upward phase propagation everywhere in the upper ocean (a radiation condition). Although the north–south scale of the imposed surface w-field was broad, the significant response was strongly equatorially trapped and showed an oscillatory structure in the vertical, just as in the observations.

In an effort to understand better how wind stress enters the equatorial ocean and to explore further the vertical structures that might be possible in stratified viscid equatorial oceans, Moore (unpublished) has studied the simplest linear model that includes the effects of continuous stratification and vertical mixing on an equatorial β-plane. The buoyancy frequency N is taken as constant, constant eddy coefficients for vertical mixing of heat κ and momentum ν are used, and, for convenience, unit Prandtl number is assumed ($\nu = \kappa$). The ocean is laterally unbounded and infinitely deep. The simplest problem to treat is the analog of the Yoshida jet, in which the system is driven by a uniform zonal wind stress τ started impulsively at $t = 0$. The problem as posed has a natural or canonical scaling. This means that for suitable choices of velocity scale U, time scale T, horizontal length scale L, and depth scale H, the resulting nondimensional equations contain no parameters. The scales are

$$L = (\nu N^2/\beta^3)^{1/2},$$

$$T = (\nu\beta^2N^2)^{-1/5},$$

$$H = (\nu^2/\beta N)^{1/5},$$

$$U = \tau(\beta N\nu^3)^{-1/5}.$$

(6.3)

Note that equations (6.3) are much less dependent on ν than are equations (6.1), essentially because here the depth scale is no longer an externally set constant! This weak dependency on ν is a characteristic advantage that all stratified models have over their homogeneous counterparts. For $N = 2 \times 10^{-3}\,\text{s}^{-1}$, $\nu = 20$ cm^2 s, and $\tau = 1$ dyn cm^{-2}, the typical values are $L = 60$ km, $T = 8$ days, $H = 40$ m, and $U = 2$ m s^{-1}. Figures 6.7A–6.7C show (y, z)-profiles of the zonal velocity u at times $t = 0.25$, 1.0, and 5.0 in Moore's model (the equator is at the right). The ranges are $0 \le y \le 5$ positive to the left and $0 \le z < 10$ positive down. Right on the equator in this x-independent model, the zonal velocity is simply governed by downward diffusion of momentum: $u_t = \nu u_{zz}$. The contour plot at time $t = 0.25$ shows that initially this balance is nearly true everywhere. At later times, the Coriolis effects have a distinct influence on the solution. The equatorial jet is well developed by $t = 1$. The solution serves to illustrate typical time and space scales of equatorial processes, as well as to point out their dependence on model parameters. Moreover, the model clearly suggests that the diffusion of zonal momentum into the deep ocean may play an important role in equatorial dynamics. However, in this x-independent and bottomless model the jet continues to intensify and deepen indefinitely. The only way to reach a steady state is to require a non-slip bottom on the ocean or to allow zonal pressure gradients, either by adding zonal structure to the wind field or by introducing boundary effects.

In the past 2 years, several fully three-dimensional and continuously stratified ocean models have been used to study wind-driven equatorial ocean circulation. The numerical models of Semtner and Holland (1980) and Philander and Pacanowski (1980a,b) are nonlinear. The analytical model of McCreary (1980) is linear; it can be regarded as an extension of the Lighthill model that allows the diffusion of heat and momentum into the deeper ocean, and also as an extension of the Stommel model into a stratified ocean. All three models are remarkably successful in reproducing many of the observed features of the Equatorial Undercurrent. For example, figure 6.8 [taken from McCreary (1980)] shows the flow field in the center of the ocean basin (10,000 km wide), where the zonal wind stress reaches a maximum (−0.5 dyn cm^{-2}). The model Equatorial Undercurrent is situated in the main thermocline beneath a surface mixed layer (75 m). The width and depth scales, as well as the speed, of the zonal flow are realistic. In addition, the pattern of meridional circulation resembles quite well the classic pattern suggested by Cromwell (1953); note that there is a strong convergence of fluid slightly above the core of the Equatorial Undercurrent, strong surface upwelling, and weaker downwelling below the core. The presence of
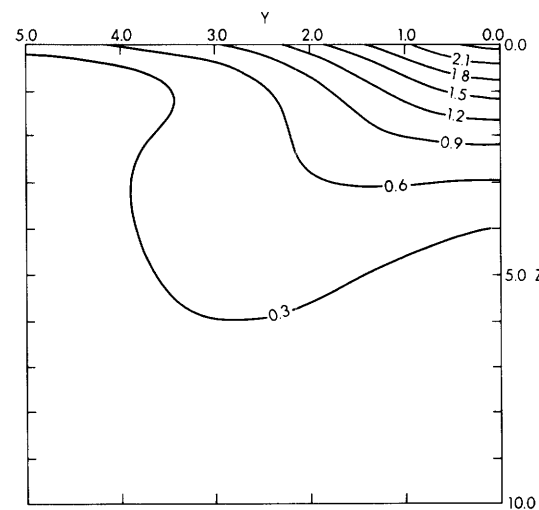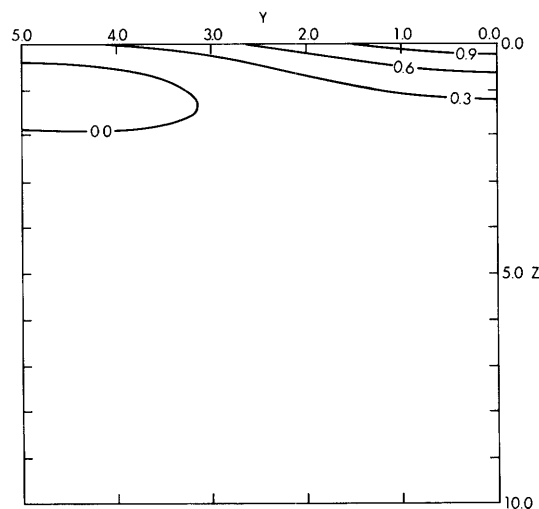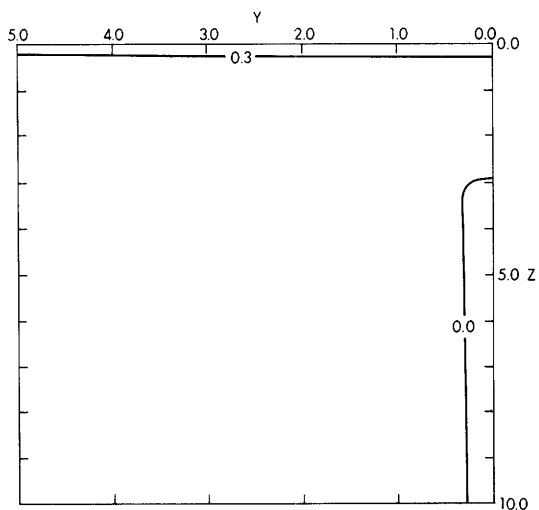
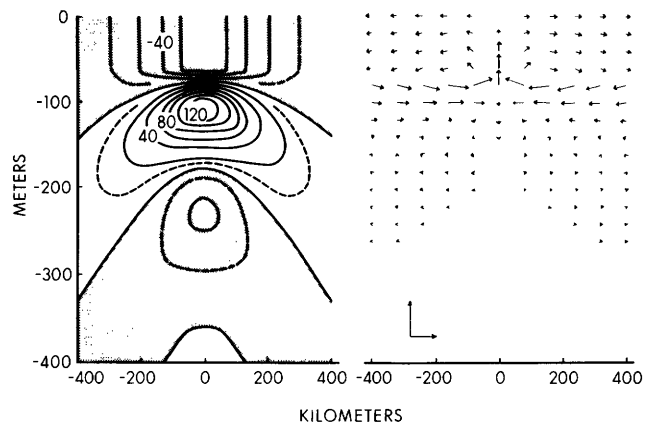A. Leetmaa, J. P. McCreary, Jr., and D. W. Moore

Figure 6.8 Vertical sections of zonal velocity (left panel) and meridional circulation (right panel) at the center of the ocean basin. The contour interval is 20 cm s^{-1}; dotted contours are ±10 cm s^{-1}. Calibration arrows in the lower left corner of the right panel have amplitudes 0.005 cm s^{-1} and 10 cm s^{-1}, respectively. (After McCreary, 1980.)

zonal baroclinic pressure gradients and the diffusion of momentum into the deep ocean are crucial for the development of this undercurrent. In fact, at the equator the balance of terms is simply $p_x = (\nu u_z)_z$. Just as in the x-independent model discussed in the preceding paragraph, stratification weakens considerably the dependence of the solution on ν. It is this property that allows a realistic undercurrent to be generated for a wide range of choices of ν. The success of the linear model suggests that nonlinearities are not essential for maintaining the Equatorial Undercurrent. They apparently act only to modify the linear dynamics, not to destroy it.

6.4 Discussion

Observations of the equatorial oceans during the past 30 years have shown the existence of surprisingly strong subsurface currents and greatly increased our knowledge of the mean structure and time variability of the surface flows. Zonal currents, both surface and subsurface, tend to occur as narrow jets several hundred kilometers wide, several hundred meters deep, and thousands of kilometers long. The observations also suggest that many tropical ocean events are remotely forced. A prime example is the phenomenon of El Niño, where wind changes in the central and western Pacific are associated with strong changes in the thermal structure of the eastern Pacific.

Perhaps because the signal-to-noise ratio is so large, theroeticians have had remarkable success in providing explanations for many equatorial phenomena. All the models suggest that stratification is an essential ingredient in equatorial dynamics. Width, depth, and time scales of model response are all intimately related to

Figure 6.7 (y, z)-contour plots of zonal velocity u in x-independent stratified spin-up on an equatorial β-plane, including the effects of vertical mixing. (A) $t = 0.25$. Diffusion effects are dominant. (B) $t = 1.0$. Equatorial jet starts to develop. (C) $t = 5.0$. Jet continues to deepen.

the background buoyancy frequency distribution [e.g., see equation (6.3)]. The presence of stratification also allows the existence of swiftly propagating equatorially trapped baroclinic waves. These waves have been used to account for remotely forced events as well as the meandering of equatorial currents.

Additional experimental and theoretical work needs to be done. It is now known that the tropical ocean responds readily and coherently to large-scale low-frequency changes in the wind field. Moreover, the nature of the response depends critically on the spatial distribution of the wind field. It is important, then, to monitor the detailed structure of the wind field on the seasonal, annual, and interannual time scales. For the first time, such observations may be practical due to rapidly improving satellite technology. Long time series of the variability of the tropical ocean flow field must also be obtained. Equatorial observations made in 1979 as part of the Global Weather Experiment should add substantial new knowledge about the circulation in all three equatorial oceans. However, the duration of this experiment is too short; it will provide at most a single realization of the annual cycle.

A major advance in our understanding of equatorial dynamics occurred when simple layer models began to be studied. These models were successful because their solutions could be easily and convincingly compared with observations; the layer interface is interpretable as the motion of the pycnocline. The recent use of equatorial models with high vertical resolution suggests that other advances may soon be forthcoming. Such models can produce a much more detailed picture of the flow field, and so can be quantitatively compared to a greater degree with the observations. Obvious problems to which these models should be applied include the existence of the thermostad and the associated subsurface countercurrents and the presence of multiple jet structures at the equator. In addition, even more sophisticated models that include realistic surface mixed layers need to be developed.

A. Leetmaa, J. P. McCreary, Jr., and D. W. Moore